Photochemical & Photobiological Sciences

Accepted Manuscript

ROYAL SOCIETY OF CHEMISTRY

www.rsc.org/pps

Photochemical & Photobiological Sciences

Photochemical & Photobiological Sciences

Dynamic Article Links ►

Cite this: DOI: 10.1039/c0xx00000x

www.rsc.org/xxxxxx

Full paper

Fluorescence enhancement of a fluorescein derivative upon adsorption on cellulose

Sergio G. Lopez,[a] Luis Crovetto,[a] Jose M. Alvarez-Pez[a], Eva M. Talavera[a*] and Enrique San Román[b*]

Received (in XXX, XXX) Xth XXXXXXXXX 20XX, Accepted Xth XXXXXXXXX 20XX
DOI: 10.1039/b000000x

9-[1-(2-methyl-4-methoxyphenyl)]-6-hydroxy-3H-xanthen-3-one (2-Me-4-OMe TG) is a fluorescein derivative dye whose photophysical properties show a remarkable pH dependency. In aqueous solution the fluorescence quantum yield (Φ_f) of its anionic species is nearly a hundred times higher than that of its neutral species. Such a large difference in Φ_f makes 2-Me-4-OMe TG useful as an "on-off" pH indicator. Here we report that adsorption on the surface of microcrystalline cellulose exerts a profound effect upon the photophysical properties of 2-Me-4-OMe TG. On the solid only the dye neutral species is observed and its Φ_f is 0.31 ± 0.10, which is approximately thirty times higher than the value found for the neutral species in aqueous solution (Φ_f = 0.01). 2-Me-4-OMe TG and Dabcyl (DB) were co-adsorbed on the surface of microcrystalline cellulose to study the transfer of excitation energy from the former to the latter. In the absence of the dye, the formation of DB aggregates is observed at concentrations greater than 0.34 μmol per gram of cellulose, while in the presence of 2-Me-4-OMe TG the formation of DB aggregates is thoroughly inhibited. The quenching of fluorescence of 2-Me-4-OMe TG by DB reaches efficiencies as high as 90% for the most concentrated samples.

Introduction

Dye immobilisation can have a great influence upon fluorescence quantum yields. Well-known examples of dyes whose fluorescence is enhanced upon immobilisation are Malachite Green and Auramine O. Augmenting the microviscosity of the medium increases the fluorescence quantum yields of these chromophores, reportedly through a decrease in the rotational freedom of their phenyl rings.[1] In contrast, immobilisation shows no effect upon the fluorescence quantum yields of other dyes, such as Rose Bengal,[2] Pheophorbide-a,[3] and Rhodamine 6G.[4] Moreover, the fluorescence quantum yield of cellulose-adsorbed Rhodamine 101 is lower than the corresponding value in aqueous solution.[5] Thus, additional research is needed to make general statements regarding the effect of dye immobilisation upon fluorescence quantum yields.

The supporting material used in this work is microcrystalline cellulose. It has been reported that the inner regions of the dry solid are nearly inaccessible to molecular oxygen.[6] In consequence, quenching of the adsorbed dyes by oxygen is negligible and, for this reason, room-temperature phosphorescence and room-temperature delayed fluorescence can be readily observed.[7,8] Microcrystalline cellulose consists of a relatively disordered and flabby amorphous region and of a relatively ordered and compact crystalline region. The accessibility of these two regions to the dye molecules depends upon the extent of swelling of the cellulose matrix, which is caused by the interactions with the solvent from which the dyes are being adsorbed.[9]

Because of its photophysical properties, 9-[1-(2-Methyl-4-methoxyphenyl)]-6-hydroxy-3H-xanthen-3-one (2-Me-4-OMe TG) is interesting as an energy donor for cellulose-adsorbed Förster Resonance Energy transfer (FRET) systems.[10] 2-Me-4-OMe TG (Scheme 1) is a novel Fluorescein (FL) derivative synthesised for the first time by Urano et al.[11] As recently demonstrated, the main non-radiative deactivation mechanism of FL and its derivatives is an intramolecular photoinduced electron transfer (PeT) process occurring from the phenyl ring to the xanthene moiety.[11-13] The rate of such a PeT depends on the substituents of the benzene ring, which regulate the redox potential of this group, as demonstrated by an elegant study in a series of FL derivatives, including 2-Me-4-OMe TG.[11] Due to the large difference between the fluorescence quantum yields of the 2-Me-4-OMe TG neutral and anionic species (pK_a = 5.9 in aqueous solution), this dye has been proposed as an "on-off" fluorescent probe.[10]

In this work we report on the influence of immobilisation of 2-Me-4-OMe TG on microcrystalline cellulose upon the photophysical properties of the dye, as determined through UV-visible diffuse reflectance spectroscopy, steady-state fluorescence and time-resolved fluorescence. Additionally, we present a

quantitative analysis of the fluorescence quenching of 2-Me-4-OMe TG by Dabcyl (4-((4-(dimethylamino)phenyl)azo)benzoic acid, DB), a non-fluorescent dye,[14] performed by the aforementioned techniques and by Fluorescence Lifetime

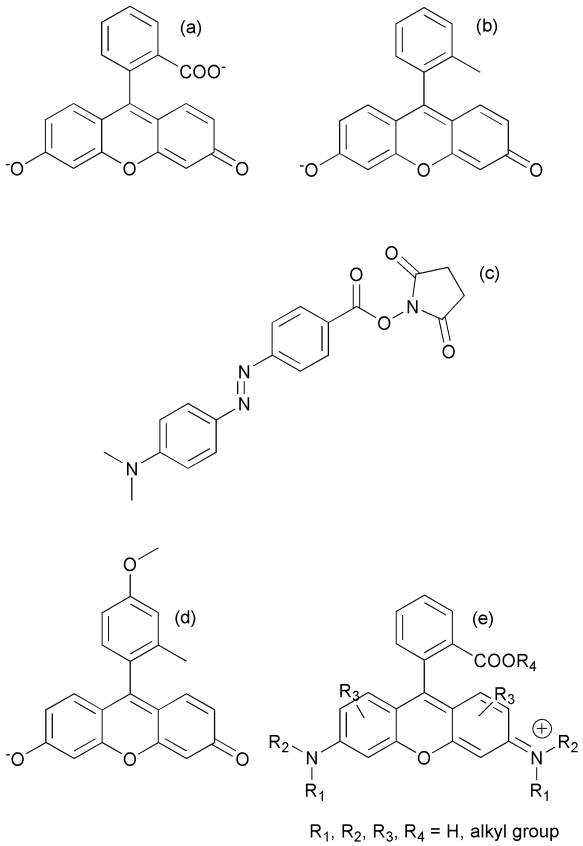

Scheme 1 Molecular structures of Fluorescein (a), 2-Me Tokyo Green (b), Dabcyl (c), 2-Me-4-OMe TG (d), and the general structure of Rhodamine dyes (e)

Imaging Microscopy (FLIM). We found that immobilisation increases the fluorescence quantum yield of the 2-Me-4-OMe TG neutral species, and that the latter species can transfer its excitation energy to DB in a highly efficient way. These findings advance the understanding of the way in which surface adsorption influences dye photophysics, facilitating the design of more efficient photoactive materials.

Experimental

Chemicals and preparation of samples

2-Me-4-OMe TG was prepared according to a previously reported procedure with 89% total yield.[10] DB (succinimidyl ester, Invitrogen), Rhodamine 6G (R6G) (laser grade, Kodak) and FL (95% purity, Sigma-Aldrich) were used as received, after checking their purity by UV/vis spectroscopy. Analytical grade ethanol, methanol and diethylether (Sigma-Aldrich) were used without further purification. Water was deionised and filtered through a 0.22 μm Millipore-Q system. Microcrystalline cellulose powder (bulk density 0.6 g mL^{-1}, pH 5-7, average particle size 20 μm, Aldrich), used as the solid support, was washed in a series of solvents (water, 1:1 water-methanol, methanol, 1:1 methanol-diethylether, diethylether) to remove impurities. Washes were performed by stirring over 2 h in each solvent or solvent mixture and by filtering after each step. The solid was finally vacuum-dried over 24 h at 40 ºC.

R6G, 2-Me-4-OMe TG, DB and FL samples were prepared by suspending microcrystalline cellulose in ethanol solutions of each dye. The ethanol was evaporated in a rotary evaporator at 40 ºC and the resulting samples were vacuum-dried over 24 h at 40 ºC. The combined 2-Me-4-OMe TG–DB samples were prepared in two steps: (1) 2-Me-4-OMe TG was adsorbed onto microcrystalline cellulose; (2) varying amounts of DB were adsorbed onto the 2-Me-4-OMe TG samples prepared in step 1. In both steps, the solid was dried as previously described. Due to their hygroscopic nature, samples were dried in a vacuum oven at 40 ºC for at least 24 h prior to each measurement. All measurements were performed at (25 ± 2) ºC.

Reflectance and emission measurements

Total and diffuse reflectance spectra of optically thick layers of particles (3 mm thickness) were recorded on a Shimadzu UV-3101 scanning spectrophotometer equipped with an integrating sphere, using barium sulphate as the reference material. True reflectance spectra were calculated as described elsewhere[15] from the reflectance spectra measured both with and without an optical filter (Schott BG18, 2 mm thickness, for R6G samples and Asahi XVS0530, 1.5 mm thickness, for 2-Me-4-OMe TG, 2-Me-4-OMe TG–DB and FL samples) in front of the detector. Remission functions were calculated according to the Kubelka-Munk theory as $F(R) = (1-R)^2/2R$.[16]

Steady-state fluorescence spectra of optically thick layers were obtained in front-face arrangement on a PTI Model QM-1 spectrofluorometer. 2-Me-4-OMe TG–DB and R6G samples were excited at 460 and 500 nm, respectively. FL and 2-Me-4-OMe TG samples were excited both at 460 and 500 nm. The emission beam was passed through suitable cut-off filters (Schott GG475 or Schott OG515, 2 mm thickness) to block scattered excitation light. The spectra were corrected for the wavelength dependence of both the detector responsivity and the filter transmittance.

Front-face measurements of fluorescence decays of thin layers of particles were taken using a Fluorocube (Horiba Jobin Yvon) fluorescence lifetime spectrofluorometer. A 495-nm LED (Horiba Jobin Yvon) working at a repetition rate of 4.4 MHz, was used as the excitation source. Thin layers of particles were prepared by spreading a small amount of sample on one side of a two-sided adhesive tape, which was affixed to a glass plate. The emission wavelength (λ_{em} = 520 nm) was selected using a monochromator. To improve the signal-to-noise ratio, suitable excitation and emission filters were employed. The histogram of the instrument response function (IRF), obtained using a Ludox scatterer, was recorded until it reached 1×10^4 counts in the peak channel. Sample decays were recorded until they reached $4 \times 10^3 - 1.4 \times 10^4$ counts in the peak channel, depending on the fluorescence intensity of each sample. The FWHM of the IRF was ~880 ps.

Fluorescence lifetime images of sample specks, dispersed atop a clean glass cover slip, were recorded with a MicroTime 200 fluorescence lifetime microscope system (PicoQuant, Inc.) using the Time-Tagged Time-Resolved (TTTR) methodology.[17] The excitation source consisted of a 470-nm pulsed diode laser (LDH-P-C-470, PicoQuant), working at a repetition rate of 20.0 MHz

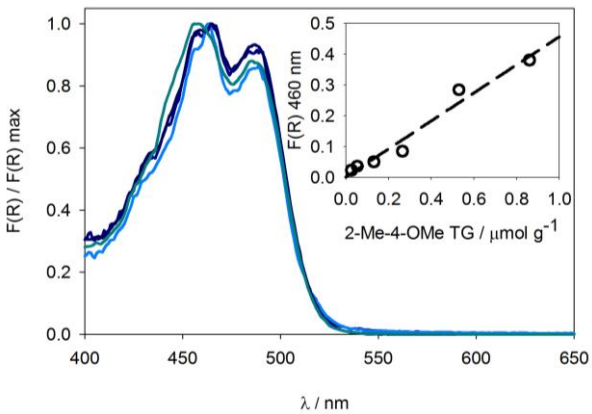

Fig. 1 Normalised remission function spectra of the 2-Me-4-OMe TG samples (for the sake of clarity, the two most diluted samples, whose spectra are relatively noisy, were omitted). Inset: remission function at 460 nm vs. 2-Me-4-OMe TG concentration.

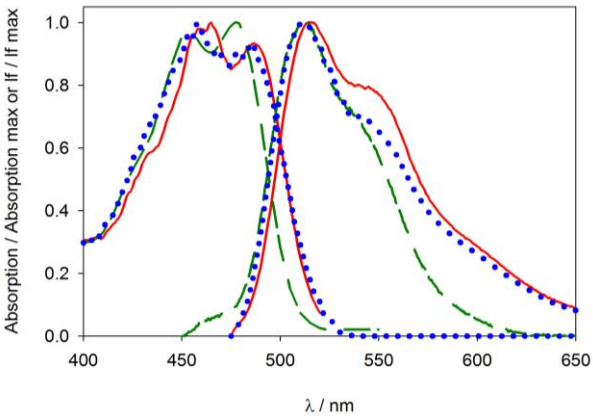

Fig. 2 Normalised remission functions and emission spectra of 2-Me-4-OMe TG (solid lines) and FL (dotted lines) on microcrystalline cellulose, and normalised absorption and emission spectra of 2-Me-4-OMe TG neutral species in aqueous solution (dashed lines). The emission spectra recorded on cellulose are corrected for reabsorption using a model described in the literature (see text).

and FWHM of 73 ps. The light beam, reflected by a dichroic mirror (510dcxr), was directed towards the oil immersion objective (1.4 NA, 100×) of an inverted microscope system (IX-71, Olympus). The collected fluorescence light was filtered by the foregoing dichroic mirror, as well as by a long-pass HP500LP filter (AHF/Chroma), and focused onto a confocal aperture. The light which passed through this confocal aperture reached a 50/50 beam splitter, which divided the fluorescence into two equally-intense beams, each of which was directed towards a separate single-photon avalanche diode (SPCM-AQR, Perkin Elmer). The data acquisition was performed using a Timeharp 200 TCSPC module (PicoQuant, GmbH).

Results and discussion

Solid samples containing 0.03–0.86 μmol g^{-1} 2-Me-4-OMe TG were prepared as described in the Experimental section. As shown in Fig. 1, the shape of the remission function spectra of these samples is independent of dye loading. The inset of Fig. 1 also shows that the 2-Me-4-OMe TG absorption maximum at 460 nm increases linearly with dye concentration. These observations indicate that 2-Me-4-OMe TG does not form aggregates within the studied concentration range.

Table 1 Fluorescence quantum yields of the 2-Me-4-OMe TG samples

[2-Me-4-OMe TG] / μmol g^{-1}	Φ_{obs} (460 nm)[a]	Φ_{obs} (500 nm)[a]	Φ_f[b]
0.03	0.18	0.20	0.21
0.05	0.27	0.28	0.31
0.13	0.36	0.33	0.41
0.27	0.26	0.22	0.31
0.53	0.28	0.25	0.32
0.86	0.27	0.22	0.31

[a] Observed fluorescence quantum yield; [b] True fluorescence quantum yield calculated from Φ_{obs} (460 nm) (see text)

Fig. 2 shows the absorption and emission spectra of 2-Me-4-OMe TG adsorbed on cellulose. The emission spectra were corrected for reabsorption by means of a previously reported procedure.[18] Because these spectra are similar to the corresponding spectra of the 2-Me-4-OMe TG neutral species in aqueous solution,[10] the local pH at the cellulose matrix must be low. To confirm this assertion, a sample containing 0.10 μmol g^{-1} FL was prepared. FL is a widely used pH indicator,[19-21] whose pK_a for the monoanion-dianion equilibrium in aqueous solution is 6.4.[22] Both the remission function and the emission spectra of the FL sample, which correspond to the monoanionic species, are shown in Fig. 2. The low local pH of the matrix may be attributed to the procedure by which microcrystalline cellulose is obtained.[23-24] Additionally, the interaction with the solid causes bathochromic shifts in both the absorption and the emission spectra of 2-Me-4-OMe TG, though the shift observed in the emission spectrum is slight. An R6G sample (0.32 μmol g^{-1}) prepared in the same way as the 2-Me-4-OMe TG samples was used as a reference to obtain the observed fluorescence quantum yields, Φ_{obs}, of the 2-Me-4-OMe TG and FL samples. Φ_{obs} values were calculated using the following equation:[18]

$$\Phi_{obs} = \Phi_{obs}^{R} \frac{J(1-R_{t,\lambda_0}^{R})I_0^{R}}{J^{R}(1-R_{t,\lambda_0})I_0} \quad (1)$$

in which I_0 is the incident photon flux; J is the emission intensity, obtained as the integrated area under the fluorescence spectrum; and $R_{t,\lambda 0}$ is the total reflectance at the excitation wavelength. Superscript R denotes reference. To obtain Φ_{obs} at 500 nm, both the sample and the reference were excited at the same wavelength and the incident photon flux ratio was internally set to unity by the instrument. In contrast, to obtain Φ_{obs} at 460 nm the sample and the reference were excited at different wavelengths (460 and 500 nm, respectively), and the ratio was obtained from the spectral distribution of the spectrofluorometer excitation channel.

Table 1 shows Φ_{obs} values obtained for the 2-Me-4-OMe TG samples on excitation at 460 and 500 nm. They are influenced by inner filter effects; the true fluorescence quantum yields, Φ_f, devoid of reabsorption artifacts were calculated from Φ_{obs} (460 nm) as reported elsewhere.[18] Almost identical values were determined from Φ_{obs} (500 nm) (not shown). Within the experimental error, Φ_f values remain constant as concentration varies. Its average, $\Phi_f = 0.31 \pm 0.10$, is approximately thirty times

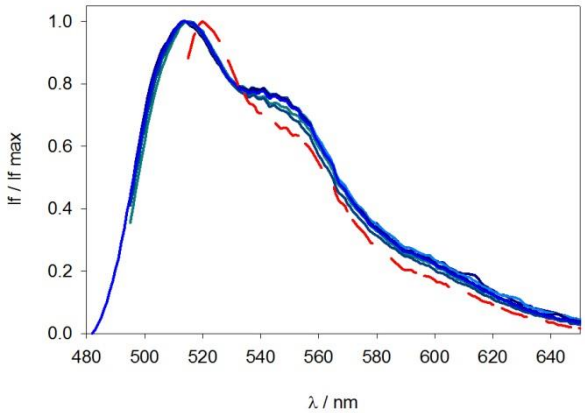

Fig. 3 Fluorescence spectra of the 2-Me-4-OMe TG samples recorded exciting at 430, 440, 450, 460, 470, 480 (solid lines) and 500 nm (dashed line). Spectra are normalised and corrected for reabsorption.

higher than the fluorescence quantum yield of the 2-Me-4-OMe TG neutral species in aqueous solution (Φ_f = 0.01).[10] In contrast a sample containing 0.10 μmol g^{-1} of FL has a value of Φ_f = 0.2, which is in the order of the value obtained for the monoanionic species in aqueous solution (Φ_f = 0.37).[25] It is noteworthy that, despite the relatively high experimental errors associated with the values shown in Table 1, it can be concluded that Φ_f for the 2-Me-4-OMe TG neutral species on cellulose is markedly different from the corresponding value in aqueous solution. In order to rule out any contribution from the 2-Me-4-OMe TG anion (Φ_f = 0.84)[10] to the fluorescence of the samples, emission spectra at different excitation wavelengths were registered. In the case of a mixture between the anionic and neutral species of 2-Me-4-OMe TG, the emission spectra of the samples should depend strongly on the excitation wavelength. Despite a red-edge effect observed when exciting at 500 nm, it is evident from Fig. 3 that the emission spectra are independent of the excitation wavelength. Consequently, the presence of the anion can be ruled out. Further support for this statement is provided by the similarity of the Φ_{obs} values obtained at two different excitation wavelengths (see Table 1). Therefore, it must be concluded that the high Φ_f obtained on cellulose is caused by the interaction with the solid, namely by one of the following scenarios:

1) The immobilisation of the phenyl group. A similar fluorescence enhancement upon adsorption was observed for Auramine O (AO, bis[4-(dimethylaminophenyl)]methylide ammonium chloride, also known as basic yellow 2 and as C.I. 41000). For AO adsorbed on microcrystalline cellulose, Φ_f = 0.35, whereas for AO in solutions of non-viscous solvents (such as water, ethanol, propanol and butanol), $\Phi_f \leq 10^{-3}$.[9] The fluorescence quantum yield of AO depends on the rotational freedom of its phenyl groups. Thus, in glycerol, a highly viscous medium, the fluorescence quantum yield of AO (Φ_f = 0.03 at 10 ºC) is greater than in media of lower viscosity.[26] The high fluorescence quantum yield of AO on cellulose has been ascribed to an interaction between the matrix and the phenyl groups of the dye.[1,9] A similar interaction may take place between the matrix and the phenyl group of 2-Me-4-OMe TG. This group is directly related to the rate of non-radiative deactivation of 2-Me-4-OMe TG because it is involved as an electron donor in a PeT to the xanthene chromophore.[11] This electron transfer is responsible for the non-radiative deactivation of FL and its derivatives.[12] Its rate of occurrence depends upon the redox potential of the phenyl group,[11,12] which is regulated by substituents.[7,9] The probability of an intramolecular electron transfer is minimal for FL and 2-Me Tokyo Green (2-Me TG) (Scheme 1), in which the substituents of the phenyl group are a carboxylic acid and a methyl group, respectively.[11] The fluorescence quantum yield of 2-Me-4-OMe TG on cellulose is similar to the fluorescence quantum yields in aqueous solution of the 2-Me TG neutral species ($\Phi_f \approx 0.32$)[11] and the FL monoanionic species. Song et al. demonstrated that the probability of PeT from a carbazole substituent to the xanthene chromophore of FL, depends on the relative orientation of the donor and acceptor moieties. If the carbazole substituent and the xanthene chromophore adopt a "face-to-face" disposition, the rate of PeT is maximised, whereas if the disposition is "shoulder-to-shoulder" the rate of electron transfer is minimized.[27] Hence, the relative dispositions of the phenyl group and the xanthene chromophore on 2-Me-4-OMe TG may be important. The immobilisation of the phenyl group, resulting from the interaction between 2-Me-4-OMe TG and the cellulose, could hinder the adoption of the most favourable disposition for electron transfer, enhancing the fluorescence quantum yield of the dye. The immobilisation of the phenyl group could also hinder the charge transfer process if this process involves the formation of a twisted intramolecular charge transfer (TICT) state, thereby increasing the fluorescence quantum yield of 2-Me-4-OMe TG.[28]

2) The formation of H-bonds involving the oxygen atom of the methoxy group. The presence of two non-bonding electron pairs on the oxygen of the methoxy substituent increases the electron density on the phenyl ring, therewith enhancing the probability of radiationless deactivation through electron transfer from the phenyl ring to the xanthene ring system. A hydrogen bond involving the methoxy group would localise these non-bonding electron pairs on the methoxy group. This would hinder the foregoing electron transfer process, resulting in an increase in Φ_f. Such a H-bond may be formed more easily in cellulose than in water considering the possibility of hydrophobic interactions between the methoxy group and the polymer matrix. Likewise, diethylamino groups of Rhodamine dyes form H-bonds more easily with alcohols than with water due to hydrophobic interactions between the alcohols and the ethylamino groups.[29-32] The existence of H-bonds involving the oxygen of the methoxy substituent is well documented.[33-36]

3) The low polarity of the cellulose. Using the $E_T(30)$ scale,[37] Iriel has shown that the polarity of the cellulose is similar to that of dichloromethane.[5] This result is concordant with the low dielectric constants reported for dry paper (ε = 1.3−1.8) and other cellulosic materials (ε = 1.3−2.9).[38] A low-polarity medium lessens the probability of intramolecular electron transfer.[39] This effect should enhance the fluorescence quantum yield of 2-Me-4-OMe TG.

The various scenarios could be operating simultaneously. Hence, further experiments are required to unravel the origin of the fluorescence enhancement.

The fluorescence decays of the 2-Me-4-OMe TG samples were best fit by a double exponential function with lifetimes τ_1 = 2.58 ± 0.50 ns (α_1 = 0.42 ± 0.21) and τ_2 = 4.49 ± 0.34 ns (α_2 = 0.58 ± 0.22). As an example, Figure 4 shows the fluorescence decay of a

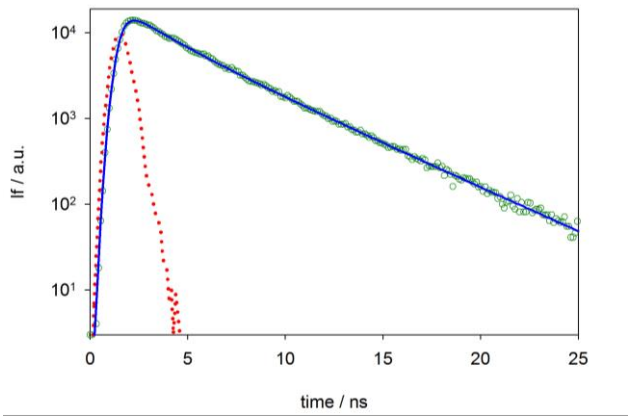

Fig. 4 Fluorescence decay of a sample containing 0.10 μmol g^{-1} 2-Me-4-OMe TG. Circles: experimental; full line: biexponential fit (τ_1 = 1.98 ns, α_2 = 0.20, τ_2 = 4.19 ns, α_1 = 0.80, χ^2 = 1.04); dotted line, IRF. λ_{ex} = 495 nm; λ_{em} = 520 nm.

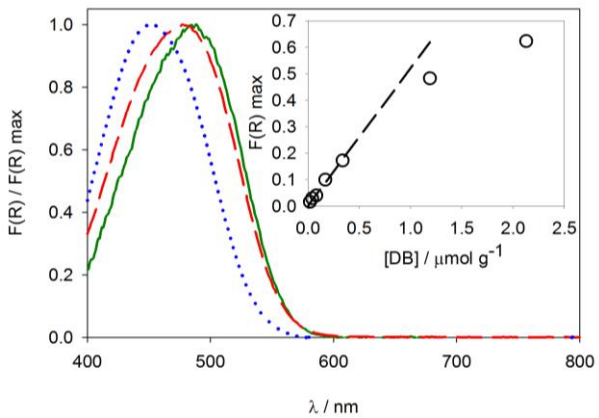

Fig. 5 Normalised remission functions of samples containing 0.09 (solid line) and 2.13 (dashed line) μmol g^{-1} DB and the absorption spectrum of a 3.88 μM DB ethanolic solution (dotted line). Inset: F(R) maximum vs. DB concentration.

2-Me-4-OMe TG sample containing 0.10 μmol g^{-1} of dye. Both τ_1 and τ_2 differ from the lifetimes obtained in solution for the 2-Me-4-OMe TG neutral (0.195 ± 0.003 ns) and anionic (3.71 ± 0.003 ns) species.[10] Therefore, τ_1 and τ_2 must be attributed not to a mixture of these species but to the occurrence of different microenvironments in the cellulose support. Recently, Duarte et al. used the exponential series method to analyse the fluorescence decay of Phloxine B adsorbed on microcrystalline cellulose. They found two distinct lifetime populations centred at 0.7 and 2.5 ns, which were assigned, respectively, to Phloxine B entrapped in the amorphous and crystalline regions of the cellulose.[7] Similarly, Rodriguez et al. reported a bimodal phosphorescence lifetime distribution for Eosin Y adsorbed on microcrystalline cellulose. This bimodal distribution consisted of lifetime populations centred at 0.76 and 2.97 ms, which were assigned, respectively, to Eosin Y present in the amorphous and crystalline regions of the cellulose.[8] Therefore, it seems reasonable to conclude that the shorter lifetime found herein for 2-Me-4-OMe TG adsorbed on microcrystalline cellulose, τ_1 = 2.58 ± 0.50 ns, corresponds to the emission of dye molecules present in the amorphous regions, where the relatively lax structure of the polysaccharide matrix would allow for larger non-radiative deactivation rates. In

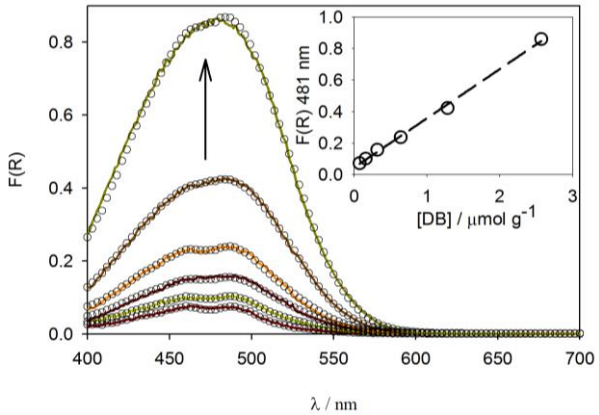

Fig. 6 Experimental (solid line) and reconstructed (circles) remission functions of the 2-Me-4-OMe TG–DB samples (2-Me-4-OMe TG concentration = 0.10 μmol g^{-1}). The arrow indicates increasing DB loading. Inset: F(R) at 481 nm vs. DB concentration.

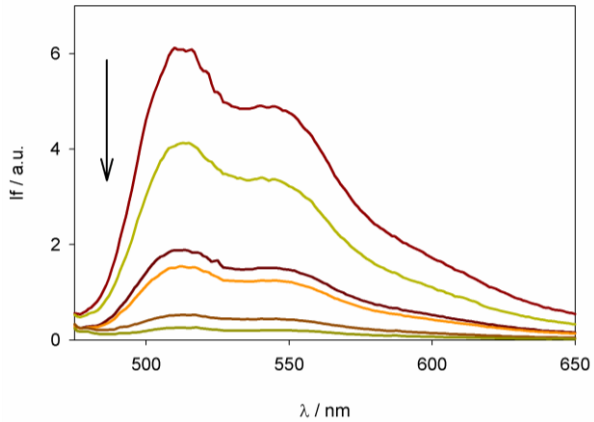

Fig. 7 Emission spectra, corrected for reabsorption, of the 2-Me-4-OMe TG–DB samples. λ_{ex} = 460 nm. A small emission from cellulose was subtracted after correction. The arrow indicates increasing DB loading.

contrast, the longer lifetime, τ_2 = 4.49 ± 0.34 ns, can be assigned to dye molecules adsorbed on the crystalline regions, in which the compact structure of the matrix would lower the chance of non-radiative deactivation.

Samples containing 0.02–2.13 μmol g^{-1} DB were prepared. As shown in Fig. 5, the remission function spectrum of DB on cellulose has a maximum at 485 nm, which shifts to 475 nm at high concentrations. This shift is accompanied by hypochromism (see inset of Fig. 5). These changes are attributed to DB aggregation. In ethanolic solution, DB has an absorption maximum at 450 nm; thus, the adsorption-associated bathochromic shift (≈ 35 nm) is quite large, meaning that the change between ground-state and first-singlet-excited-state dipole moments is also large. Because DB exhibits negative solvatochromism (as ethanol is more polar than cellulose), it can be concluded that the first singlet excited state of this dye is less polar than its ground state.

DB is a potential acceptor for the excitation energy of 2-Me-4-OMe TG. The use of a non-fluorescent acceptor facilitates the analysis of the donor fluorescence, allowing a straightforward determination of the quenching efficiency, especially if the acceptor concentration is much greater than the donor

concentration. High acceptor concentrations are needed to obtain significant energy transfer efficiencies, whereas low donor concentrations prevent energy migration and further simplify the analysis.[40-44] Samples containing 0.10 μmol g^{-1} 2-Me-4-OMe TG and 0.08–2.57 μmol g^{-1} DB were prepared. 2-Me-4-OMe TG inhibits DB aggregation in the whole concentration range, as it can be demonstrated by the following arguments: 1) the remission functions of 2-Me-4-OMe TG–DB samples (Fig. 6) can be reconstructed by combination of the spectra of pure 2-Me-4-OMe TG and pure low-concentration DB; 2) The inset of Fig. 6 shows that the value of the remission function at 481 nm (the monomeric DB absorption maximum) increases linearly with DB concentration. Likewise, previous works reported the inhibition of Methylene Blue (MB) aggregation both by Rhodamine 101 (R101)[45] and Pheophorbide A (PheoA).[46] The origin of this inhibition remains uncertain. However, considering that it has been observed between chromophores of the same electric charge (R101 and MB) and between chromophores of opposite electric charges (PheoA and MB), it can be concluded that dye-to-dye hydrophobic interactions play an important role in the inhibition of aggregation. Noteworthy, the effect is present at very low concentrations of 2-Me-4-OMe TG.

Fig. 7 shows the emission spectra of the 2-Me-4-OMe TG–DB samples corrected for reabsorption. Spectra decrease in intensity maintaining their shape on increasing DB concentration. This decrease can be attributed both to inner filter effects and to fluorescence quenching of 2-Me-4-OMe TG by DB. Quenching efficiencies, E, were calculated using the following equation:[4]

$$\frac{I_{\mathrm{F,D}}}{I^{*}_{\mathrm{F,D}}} = \frac{(1-R)\alpha_{0\mathrm{D}}}{(1-R^{*})\alpha^{*}_{0\mathrm{D}}} \frac{(1-\Phi_{\mathrm{D}}P^{*}_{\mathrm{DD}})(1-E)}{[1-\Phi_{\mathrm{D}}(1-E)P_{\mathrm{DD}}]} \qquad (2)$$

in which $I_{\mathrm{F,D}}$ is the donor fluorescence intensity (515 nm), R is the total reflectance of the sample at the excitation wavelength (460 nm), Φ_{D} is the donor fluorescence quantum yield (0.31), $\alpha_{0\mathrm{D}}$ is the fraction of the absorbed radiation exciting the donor, and P_{DD} is the probability that the donor fluorescence is reabsorbed by the donor. The asterisk indicates absence of quencher (DB). All quantities can be obtained from remission function and fluorescence data.[4] Experimental efficiencies are shown in Table 2 as a function of concentration. Values in the order of 90 % are found at the highest DB concentration.

To ascertain the nature of the quenching time resolved experiments were performed. Fluorescence decays (FDs, see Fig. 8) and fluorescence lifetime distributions (FLDs, see Fig. 9) were measured for 2-Me-4-OMe TG–DB samples. FDs were determined by single photon counting on samples comprising many microcrystalline cellulose particles and therefore represent bulk averages, while FLDs were determined by FLIM over a few particles, scanning the sample over a surface of nearly 80 μm × 80 μm with a confocal volume of about 1 fL. The confocal volume is such that a fraction of a particle is sampled, containing in average 1500 2-Me-4-OMe TG molecules and many more DB molecules in most of the samples. The analysis routine (fast FLIM) consists in building up a TCSPC histogram for each pixel and calculating an average lifetime as $\Sigma_i N_i t_i / \Sigma N_i$, where N_i is the number of photons arrived at the channel centred at time t_i. When each pixel contains at most one active molecule decaying exponentially, this procedure yields the characteristic lifetime of its excited state. For many molecules, the same procedure yields an intensity average lifetime, obtained in general and for a multiexponential decay as:[1]

Table 2 Average fluorescence lifetimes of the 2-Me-4-OMe TG–DB samples (ns)

[DB] (μmol g^{-1})	intensity average (eq. 3)	intensity average (FLIM)	amplitude average (eq. 4)	E exptl. (eq. 2)	E calculated (eq. 5)
0.00	3.9	4.0	3.7	-	-
0.08	3.8	-	3.6	0.08	0.05
0.16	3.7	-	3.4	0.14	0.10
0.32	3.6	-	3.2	0.32	0.12
0.64	3.6	3.7	3.2	0.61	0.14
1.28	3.3	3.3	2.8	0.60	0.26
2.57	3.0	3.0	2.4	0.91	0.36

Uncertainty in lifetimes can be estimated as ± 0.2 ns.

$$<t>_{\mathrm{int}} = \int_0^{\infty} tI(t)\mathrm{d}t \Big/ \int_0^{\infty} I(t)\mathrm{d}t \rightarrow \sum_i \alpha_{\mathrm{i}}\tau_{\mathrm{i}}^2 \Big/ \sum_i \alpha_{\mathrm{i}}\tau_i \qquad (3)$$

where $I(t)$ is the fluorescence intensity as a function of time and α_{i} and τ_{i} the amplitudes and decay times of the multiexponential expansion. Intensity average lifetimes differ from amplitude average lifetimes, obtained in general and for a multiexponential decay as:

$$<t>_{\mathrm{amp}} = \int_0^{\infty} \frac{I(t)}{I(0)} dt \rightarrow \sum_{\mathrm{i}} \alpha_{\mathrm{i}}\tau_{\mathrm{i}} \Big/ \sum_{\mathrm{i}} \alpha_{\mathrm{i}} \qquad (4)$$

Various lifetime averages are shown in Table 2. The FDs shown in Figs. 4 and 7 were approximated by biexponentials to obtain $<t>_{\mathrm{int}}$ and $<t>_{\mathrm{amp}}$ from eqs. (3) and (4) respectively. Adding a third exponential yielded similar lifetime averages, within the experimental error interval quoted in Table 2, and therefore the biexponential approximation was retained. Integration of the decay function through eq. (3) (not shown) yielded also similar intensity average lifetimes. In all these calculations decays after 2 ns (see Figs. 4 and 8) were considered. For all samples, the weak autofluorescence of cellulose was insignificant in comparison with the dye fluorescence. Mean intensity average lifetimes, obtained from the FLDs shown in Fig. 9 as the centre of mass of each distribution, were also coincident with $<t>_{\mathrm{int}}$ values. Multiexponential analysis through deconvolution of whole fluorescence histograms (not shown) did not show any decrease of average lifetimes, as it would be expected if a rapid decay component masked by the IRF existed. Taking into account the methodologies employed to estimate the lifetimes and the magnitude of the FWHM of the IRFs (880 and 73 ps for TCSPC and FLIM experiments, respectively) a lower bound of ca. 100 ps can be set for the lowest detectable decay.

The fact that average lifetimes shorten when acceptor concentration increases is consistent with the occurrence of dynamic, i.e. Förster energy transfer. However, the rather small dependence of average lifetimes with concentration obtained by the methods so far discussed is not compatible with quenching efficiencies reaching about 90 %. In fact, as it may be seen in Table 2 Förster energy transfer efficiencies, calculated from amplitude average lifetimes as:[47]

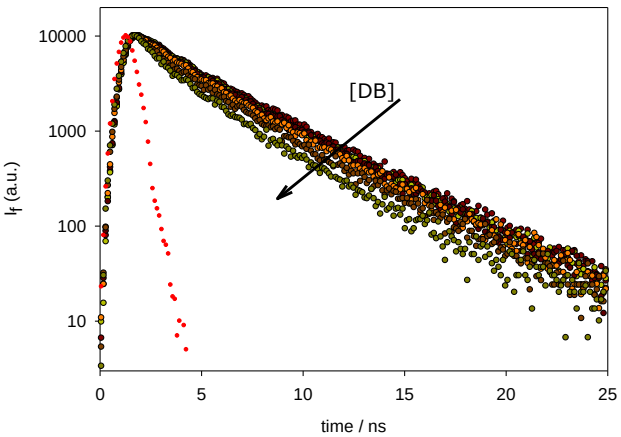

Fig. 8 Fluorescence decays of the 2-Me-4-OMe TG–DB samples (solid lines) and IRF (dotted line). λ_{ex} = 495 nm; λ_{em} = 520 nm.

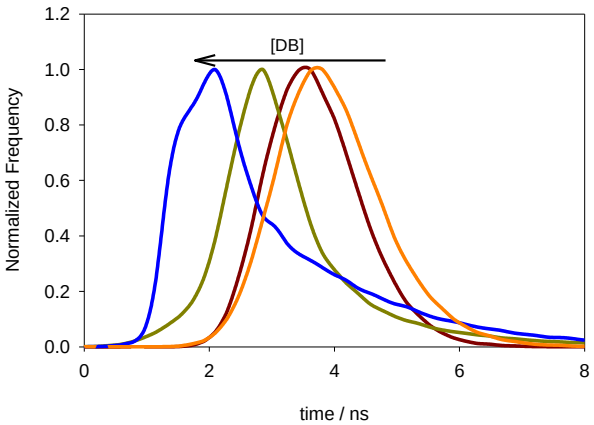

Fig. 9 Fluorescence lifetime distributions of the 2-Me-4-OMe TG and 2-Me-4-OMe TG–DB samples. From left to right: 2.57, 1.28, 0.64, and 0 μmol DB g^{-1}. All samples contain 0.10 μmol g^{-1} 2-Me-4-OMe TG.

$$E = 1 - \frac{\int_0^\infty I(t)dt}{\int_0^\infty I^0(t)dt} = 1 - \frac{<t>_{amp}}{<t>^0_{amp}} \quad (5)$$

where superscript "0" means absence of acceptor, hardly reach 40 % at the highest DB concentration. The difference between E values obtained from eqs. (2) and (5) might be attributed to other quenching routes but components of a Förster decay below 100 ps would also remain undetectable and cannot be discarded. For that reason, E values calculated through eq. (5) have to be considered as lower bounds to the real energy transfer efficiencies. It should be noticed that this equation, applied usually to donor-acceptor pairs, is valid also for donors interacting with multiple acceptors.

The interpretation of Fig. 9 is not straightforward. Owing to the occurrence of different microenvironments in microcrystalline cellulose, bimodal FLDs as those found in the analysis of FDs of phloxine B can be expected.[7] However, even in such a case and given the magnitude of the confocal volume and the number of molecules confined in it, a sharp distribution of lifetimes would be expected if acceptor molecules were distributed evenly throughout the sample. As this is not the case, it has to be concluded that molecules distribute unevenly among microscopic domains. Moreover, the long tail observed at the highest DB concentrations shows that domains with nearly isolated 2-Me-4-OMe TG molecules coexist with domains composed by molecules surrounded by a large numbers of acceptors. In this picture, the coincidence between intensity averages obtained from eq. (3) and mean intensity averages calculated as the centre of mass of FLDs obtained by FLIM is not fortuitous, because both values measure the average lifetime of a 2-Me-4-OMe TG excited molecule irrespective of the complexity of the FLD.

A simple calculation shows that FRET is at least plausible, as a Förster radius, R_0 = 36 Å, can be estimated for the energy transfer from 2-Me-4-OMe TG to DB, considering an orientational parameter κ^2 = 0.476 (static isotropic average)[48-50] and a refractive index of n = 1.47 (glycerol). For that sake, the overlap integral was obtained by scaling the area under the remission function of DB to the absorption spectrum of the dye in ethanol, assuming equal oscillator strengths in both media. Other dye pairs adsorbed from ethanol on microcrystalline cellulose so far studied with R_0 values around 50–60 Å[51] yielded energy transfer efficiencies as a function of the acceptor concentration which could be fitted considering a surface area σ = 60 m^2 g^{-1}. Next relationship can be deduced from the usual FRET equations for the two-dimensional case:[1]

$$E = 1 - \int_0^\infty \exp\left[-x - \Gamma(2/3)\frac{[DB]}{\sigma}\pi R_0^2 x^{1/3}\right]dx \quad (6)$$

where $x = t / <t>^0_{amp}$ and Γ is the Gamma function. Owing to the complexity of the present system, eq. (6) yields only a crude approximation to the energy transfer efficiency. Considering the quoted values for R_0 and σ, an energy transfer efficiency of nearly 70 % can be computed for [DB] = 2.57 μmol g^{-1}. From the foregoing discussion, it may be concluded that FRET is at least one of the relevant quenching mechanisms for excited 2-Me-4-OMe TG and contributes to a large extent to the quenching efficiency.

Conclusions

Only the neutral form of 2-Me-4-OMe TG is present in cellulose with a fluorescence quantum yield Φ_f = 0.31 ± 0.10, thirty times higher than in aqueous solution (Φ_f = 0.01). This fluorescence enhancement can be attributed to the low polarity of cellulose, which should lessen the probability of photoinduced intramolecular electron transfer. Alternative explanations are the immobilisation of the phenyl group, and the formation of H-bonds involving the oxygen of the methoxy group. No evidence of 2-Me-4-OMe TG aggregation is found. DB, a non-fluorescent dye, was adsorbed onto microcrystalline cellulose and studied as an acceptor for the excitation energy of 2-Me-4-OMe TG. In pure DB samples, the formation of DB aggregates is associated with hypochromism, with a hypsochromic shift in the absorption spectrum. In addition, a strong negative solvatochromism was observed for DB. 2-Me-4-OMe TG was found to inhibit the aggregation of DB molecules across the entire range of concentrations. Both the 2-Me-4-OMe TG fluorescence decays and the lifetime distributions support the occurrence of a non-

radiative (Förster-type) energy transfer mechanism. For the most concentrated 2-Me-4-OMe TG–DB samples quenching efficiencies as high as 90% are obtained. A large fraction of this efficiency can be attributed to FRET from 2-Me-4-OMe TG to DB.

Acknowledgements

This work was supported by grant A/012706/07 from the Agencia Española de Cooperación Internacional (AECI). Funding from ANPCyT, CONICET and UBA is acknowledged. SGL thanks CONICET for a graduate fellowship. Special thanks are due to Guillermo Menéndez and the late Elizabeth Jares-Erijman for helping with time-resolved measurements and to Hernán Bernardo Rodríguez for helpful discussions.

Notes and references

[a] *Departamento de Fisicoquímica, Universidad de Granada, Campus de Cartuja,18071, Granada, Spain.*
[b] *INQUIMAE, Facultad de Ciencias Exactas y Naturales, Universidad de Buenos Aires, Ciudad Universitaria, C1428EHA, Buenos Aires, Argentina.*
**Authors to whom correspondence should be addressed.*
Tel.: + 34-958-243826; fax: + 34-958-244090; e-mail: etalaver@ugr.es
Tel.: + 54-11-4576-3378/80ex118; fax: + 54-11-4576-3341; e-mail: esr@qi.fcen.uba.ar

† Electronic Supplementary Information (ESI) available: [details of any supplementary information available should be included here]. See DOI: 10.1039/b000000x/

‡ Footnotes should appear here. These might include comments relevant to but not central to the matter under discussion, limited experimental and spectral data, and crystallographic data.

1 B. Valeur, in *Molecular Fluorescence*. Principles and Applications. Wiley-VCH Verlag GmbH, Weinheim, 1st edn., 2001.
2 H. B. Rodríguez, M. G. Lagorio, and E. San Román, Rose Bengal adsorbed on microgranular cellulose: evidence on fluorescent dimers, *Photochem. Photobiol. Sci*., 2004, **3**, 674-680..
3 M. G. Lagorio, E. San Román, A. Zeug, J. Zimmermann, and B. Röder, Photophysics on surfaces: Absorption and luminescence properties of Pheophorbide-a on cellulose, *Phys. Chem. Chem. Phys.*, 2001, **3**, 1524-1529.
4 S. G. López, G. Worringer, H. B. Rodríguez and E. San Román, Trapping of Rhodamine 6G excitation energy on cellulose microparticles, *Phys. Chem. Chem. Phys*., 2010, **12**, 2246-2253..
5 A. Iriel, PhD thesis, University of Buenos Aires, 2006.
6 F. Wilkinson, P. A. Leicester, L. F. Vieira Ferreira, and V. M. M. R. Freira, Photochemistry on surfaces: triplet-triplet energy transfer on microcrystalline cellulose studied by diffuse reflectance transient absorption and emission spectroscopy, *Photochem. Photobiol*.,1991, **54**, 599–608.
7 P. Duarte, D. P. Ferreira, I. F. Machado, L. F. Vieira Ferreira, H. B. Rodríguez and E. San Román, Phloxine B as a probe for entrapment in microcrystalline cellulose, *Molecules*, 2012, **17**, 1602-1616.
8 H. B Rodríguez, E. San Román, P. Duarte, I. Ferreira Machado and L. F. Vieira Ferreira, Eosin Y triplet state as a probe of spatial heterogeneity in microcrystalline cellulose, *Photochem. Photobiol*. 2012, **88**, 831-839.
9 L. F. Vieira Ferreira, A. R. Garcia, M. R. Freixo and S. M. B. Costa, Photochemistry on surfaces: solvent–matrix effect on the swelling of cellulose. An emission and absorption study of adsorbed auramine O. *J. Chem. Soc., Faraday Trans*., 1993, **89**, 1937–1944.
10 J. M. Paredes, L. Crovetto, R. R., Angel Orte, J. M. Alvarez-Pez and E. M. Talavera, Tuned lifetime, at the ensemble and single molecule level, of a xanthenic fluorescent dye by means of a buffer-mediated excited-state proton exchange reaction, Phys. Chem. Chem. Phys., 2009, **11**, 5400-5407.
11 Y. Urano, M. Kamiya, K. Kanda, T. Ueno, K. Hirose and T. Nagano, Evolution of fluorescein as a platform for finely tunable fluorescence probes, *J. Am. Chem. Soc*., 2005, **127**, 4888-4894.
12 K. Tanaka, T. Miura, N. Umezawa, Y. Urano, K. Kikuchi, T. Higuchi and T. Nagano, Rational design of fluorescein-based fluorescence probes. Mechanism-based design of a maximum fluorescence probe for singlet oxygen, *J. Am. Chem. Soc*., 2001, **123**, 2530-2536.
13 T. Miura, Y. Urano, K. Tanaka, T. Nagano, K. Ohkubo and S. Fukuzumi, Rational design principle for modulating fluorescence properties of fluorescein-based probes by photoinduced electron transfer, *J. Am. Chem. Soc.*, 2003, **125**, 8666-8671.
14 J. G. Nadeau, J. B. Pitner, C. P. Linn, J. L. Schram, C. H. Dean, C. M. Nycz, Real-Time, Sequence-Specific Detection of Nucleic Acids during Strand Displacement Amplification, *Anal. Biochem*., 1999, **276**, 177-187.
15 M. Mirenda, M. G. Lagorio and E. San Román, Photophysics on surfaces: determination of absolute fluorescence quantum yields from reflectance spectra, *Langmuir*, 2004, **20**, 3690-3697.
16 W. W. Wendlandt and H. G. Hecht, in *Reflectance Spectroscopy*, Wiley Interscience, New York, 1966, ch. 3, pp. 55–76.
17 M. Wahl, R. Erdmann, K. Lauritsen and H. J. Rahn, Hardware solution for continuous time resolved burst detection of single molecules in flow, *Proc. SPIE*, 1998, **3259**, 173-178.
18 M. G. Lagorio, L. E. Dicelio, M. I. Litter and E. San Román, Modeling of fluorescence quantum yields of supported dyes Aluminium carboxyphthalocyanine on cellulose, *J. Chem. Soc., Faraday Trans*., 1998, **94**, 419-425.
19 M. M. Wu, J. Llopis, S. Adams, J. M. McCaffery, M. S. Kulomaa, T. E. Machen, H. –P. H Moore and R. Y. Tsien, Organelle pH studies using targeted avidin and fluorescein-biotin, *Chem. Biol.*, 2000, **7**, 197-209.
20 L. Y. Ma, H. Y. Wang, H. Xie and L. X. Xu, A long lifetime chemical sensor: study on fluorescence property of fluorescein isothiocyanate and preparation of pH chemical sensor, *Spectrochim. Acta, Part A*, 2004, **60**, 1865-1872.
21 A. Nilsen, K. Nyberg and P. Camner, Intraphagosomal pH in alveolar macrophages after phagocytosis in vivo and in vitro of fluorescein-labeled yeast particles, *Exp. Lung Res*., 1988, **14**, 197-207.
22 J. Yguerabide, E. Talavera, J. M. Alvarez and B. Quintero, Steady-state fluorescent method for evaluating excited state proton reactions: application to fluorescein, *Photochem. Photobiol*., 1994, **60**, 435-441.
23 *US Pat*., 2978446, 1961.
24 *US Pat*., 3954727, 1976.
25 R. Sjöback, J. Nygren and M. Kubista, Absorption and fluorescence properties of fluorescein, *Spectrochim. Acta Part A*, 1995, **51**, L7-L21.
26 G. Oster and Y. Nishijima, Fluorescence and internal rotation: their dependence on viscosity of the medium, *J. Am. Chem. Soc*., 1956, **78**, 1581-1584.
27 A. Song, T. Wu, S. Chen, M. Zhang and T. Shen, Syntheses and photophysical properties of amphiphilic dyads of fluorescein and carbazole linked with a flexible or semi-rigid bridge, *Dyes Pigm*., 1998, **39**, 371-382.
28 M. A. Haidekker, T. P. Brady, D. Lichlyter and E. A. Theodorakis, Effects of solvent polarity and solvent viscosity on the fluorescent properties of molecular rotors and related probes, *Bioorg. Chem*., 2005, **33**, 415-425.
29 I. López Arbeloa and K. K. Rohatgi-Mukherjee, Solvent effect on photophysics of the molecular forms of rhodamine B. Solvation models and spectroscopic parameters, *Chem Phys. Lett*., 1986, **128**, 474-479.
30 F. López Arbeloa, T. López Arbeloa, M. J. Tapia Estevez and I. López Arbeloa. Photophysics of rhodamines: molecular structure and solvent effects, *J. Phys. Chem*., 1991, **95**, 2203-2208.
31 D. Magde, G. E. Rojas and P. G. Seybold, Solvent dependence of the fluorescence lifetimes of xanthene dyes, *Photochem. Photobiol*., 1999, **70**, 737-744.
32 T. López Arbeloa, F. López Arbeloa, P. Hernández Bartolomé and I. López Arbeloa, On the mechanism of radiationless deactivation of rhodamines, *Chem. Phys*., 1992, **160**, 123-130.

33 Y. Tatamitani, B. Liu, J. Shimada, T. Ogata, P. Ottaviani, A. Maris, W. Caminati and J. L. Alonso, Weak, improper, C−O•••H−C hydrogen bonds in the dimethyl ether dimer, *J. Am. Chem. Soc*., 2002, **124**, 2739-2743.

34 J. Meszko, K. Krzymiński, A. Konitz and J. Błażejowski, 2-Methylphenyl 2-methoxyacridine-9-carboxylate, *Acta Cryst*., 2002, C**58**, o157-o158.

35 J. T. Kiss, K. Felföldi, I. Hannus and I. Pálinkó, Hydrogen bonded networks of methoxy-substituted α-phenylcinnamic acids studied by spectroscopic and computational methods, *J. Mol. Struct*., 2001, **565-566**, 463-468.

36 M. Palusiak and S. J. Grabowski, Methoxy group as an acceptor of proton in hydrogen bonds, *J. Mol. Struct*., 2002, **642**, 97-104.

37 C. Reichardt, Solvatochromic dyes as solvent polarity indicators, *Chem. Rev*., 1994, **94**, 2319-2358.

38 G. A. Baum, in *Handbook of physical testing of paper*, ed. J. Borch, M. B. Lyne, R. E. Mark, C. Habeger, CRC Press, 2nd edn., 2001, vol. 2, ch. 4, pp. 369-370.

39 M. W. Holman, R. Liu, L. Zang, P. Yan, S. A. DiBenedetto, R. D. Bowers and D. M. Adams, Studying and switching electron transfer: from the ensemble to the single molecule, *J. Am. Chem. Soc*., 2004, **126**, 16126-16133.

40 D. L. Huber, Fluorescence in the presence of traps, *Phys. Rev. B*, 1979, **20**, 2307-2314.

41 C. R. Gouchanour, H. C. Anderson and M. D. Fayer, Electronic excited state transport in solution, *J. Chem. Phys*., 1979, **70**, 4254-4271.

42 R. F. Loring, H. C. Anderson and M. D. Fayer, Electronic exited state transport and trapping in solution, *J. Chem. Phys*., 1982, **76**, 2015-2027.

43 L. Kulak and C. Bojarski, Forward and reverse electronic energy transport and trapping in solution. I. *Theory*, *Chem. Phys*., 1995, **191**, 43-66.

44 S. Engström, M. Lindberg and L. B.-Å. Johansson, Monte Carlo simulations of electronic energy transfer in three-dimensional systems: A comparison with analytical theories, *J. Chem. Phys*., 1988, **89**, 204-213.

45 H. B. Rodríguez, A. Iriel and E. San Román, Energy transfer among dyes on particulate solids, *Photochem. Photobiol*., 2006, **82**, 200-207.

46 H. B. Rodríguez and E. San Román, Energy transfer from chemically attached rhodamine 101 to adsorbed methylene blue on microcrystalline cellulose particles, *Photochem. Photobiol*., 2007, **83**, 547-555.

47 P. Wu and L. Brand, Resonance energy transfer: methods and applications, *Anal. Biochem.* 1994, **218** 1-13.

48 M. D. Galanin, The problem of the effect of concentration on the luminescence of solutions, *Soviet Physics−JETP*, 1955, **1**, 317-325.

49 M. Z. Maksimov, and I. M. Rozman, On the energy transfer in rigid solutions, Optika I Spektroskopiya 1962, **12**, 606-609.

50 I. Z. Steinberg, Nonradiative energy transfer in systems in which rotatory Brownian motion is frozen, *J. Chem. Phys*., 1968, **48**, 2411-2413.

51 H. B. Rodríguez, *PhD Thesis*, University of Buenos Aires, 2009.